symmetry

IMPACT FACTOR 2.2

CITESCORE 5.4

Article

Nonlocal Effects in Asymptotically Safe Gravity

Sándor Nagy

MDPI

https://doi.org/10.3390/sym16081074

symmetry

MDPI

Article

Nonlocal Effects in Asymptotically Safe Gravity

Sándor Nagy

Department of Theoretical Physics, University of Debrecen, P.O. Box 400, H-4002 Debrecen, Hungary; sandor.nagy@science.unideb.hu

Abstract: The asymptotically safe gravity is investigated in the framework of the functional renormalization group method. The low energy region of the model can account for the cosmological behavior, where it is assumed that the nonlocal effects play a crucial role. Using the Wegner–Houghton equation it is shown that the dynamically induced bilocal term modifies the infrared scaling of the model.

Keywords: renormalization group; asymptotic safety; infrared behaviour

1. Introduction

The functional renormalization group (RG) method [1–7] teaches us that the constants of physics are not necessarily constants, they can vary. A classical example can be the Newton's constant G, which appears in the potential describing the gravitational interactions between massive bodies. However, it turned out that in the quantum theory of gravity, i.e., in the asymptotically safe gravity, G becomes a function of the observation scale k [8–10]. The asymptotically safe gravity seems to be a suitable model describing the gravitational interaction for all energy scales. Furthermore, the issue of perturbative non-renormalizability is also solved by finding an ultraviolet (UV) attractive fixed point, the Reuter fixed point in the asymptotically safe gravity, that makes all the theoretical predictions finite [11–14]. We note that besides the RG method, the asymptotic safety in gravity has been studied in Euclidean dynamical triangulations [15], in causal dynamical triangulations [16], in Regge lattice gravity theory [17] or in tensor models [18].

The asymptotically safe gravity can describe the gravitational interaction in extremely large energy scales, starting from the UV energies, down to the infrared (IR) scaling regime. The model also serves as a possible unification of gravity and quantum physics. The phase space of the model contains all the possible values of Newton's constant G_k and the cosmological constant Λ_k including the one belonging to our observations, the trajectory picked up by Nature. This trajectory spans about 60 orders of magnitude in the scale k [19,20] where the couplings should be followed, making the RG method unavoidable in the description of the asymptotically safe gravity.

The quantized version of gravity should account for the classical general relativity, including cosmological phenomena, too. In the UV regime, quantum gravity dominates, and it is characterized by the Reuter fixed point beyond the Planck scale ($k \sim 10^{27}$ eV). By lowering the RG scale we can find the scale of inflation (10^{22} eV), the classical general relativity region in the laboratory scale (10^{-5} eV), and going further towards the IR, we can find the Hubble scale (10^{-33} eV) [19,21].

We can find a significant discrepancy between the observable mass and the one obtained from observed motion for galactic systems. A possible explanation can be the existence of dark matter; however, a modification of the deep IR scaling can account for the discrepancy. As an example, a possible interacting IR fixed point can modify the evolution of G_k and Λ_k in such a way that the gravitational attraction at the cosmological scales changes making the model suitable for writing down the motion at galaxy scales [20,22]. The interacting IR fixed point is assumed to appear due to some possible new physical interactions since quantum gravity and their extension can hardly account for the new IR

Citation: Nagy, S. Nonlocal Effects in Asymptotically Safe Gravity. *Symmetry* **2024**, *16*, 1074. https://doi.org/10.3390/sym16081074

Academic Editors: Kazuharu Bamba and Stefano Profumo

Received: 18 July 2024
Revised: 5 August 2024
Accepted: 16 August 2024
Published: 19 August 2024

scalings. It is also an accepted belief that the new deep IR scaling should come from nonlocal interactions. However, nonlocal couplings can come not only from new interactions, but they may also rise from the original model due to the effect of the RG blocking steps. This mechanism comes from the recognition, that there is a nontrivial saddle point that dominates the RG blocking step [23], and produces a tree-level evolution to the nonlocal part of the potential. The rising of nonlocal couplings can modify the IR behavior of gravity, implying that the nonlocality can appear without introducing new physics.

In this work, we determine the evolution of the nonlocal (usually bilocal) potential and calculate its effect on IR physics. We use the Wilsonian approach of finding the evolution equation of the bare action (oppositely the usual way of finding the evolution of the effective average action) by the Wegner–Houghton equation [24]. This approach can also be used to investigate quantum gravity [25–27]. The sharp cutoff enables us to find the saddle point of the eliminated modes analytically. We derive the evolution equation for the bilocal potential and follow the evolution of the bilocal coupling. We show that the cosmological constant initiates the evolution of the bilocal coupling. In this approach, we do not assume the existence of new interactions in the IR region, but we consider the nonlocal effects in quantum gravity that have not been investigated yet.

We look for the possible IR fixed point of quantum gravity including its bilocal potential evolution. In order to clarify the IR behavior we change the coupling Λ_k and the cutoff scale in such a way that there are no singularities in the new flow equations [28,29]. We refer to these new flow equations as transformed ones. By using this technique a possible IR fixed point is found in asymptotically safe gravity [30]. The same IR fixed point was found in [31]. We should note that this fixed point differs from the one in [20], because the latter corresponds to interacting IR fixed point, with nonvanishing Newton's constant.

First, we consider the traditional form of asymptotically safe gravity using the Wetterich equation [32] and look for the fixed points and the corresponding exponents. Then, the transformed equations are investigated. We repeat these steps to the conformally reduced quantum gravity, where the conformal part of the metric can only fluctuate [20,22,33–35]. In the last step we let the bilocal coupling evolve, also in the framework of the conformally reduced quantum gravity and compare the evolution of the local evolution with the bilocal one. The great advantage of this method is the lower technical complexity since there is no need for gauge fixing. In the traditional treatment of gravity, the background field method is very sensitive to the choice of the gauge [36,37]. Usually, the background harmonic gauge is used, which is very popular since certain simplifications can be made. The conformally reduced gravity is practically a scalar theory in curved spacetime with a negative kinetic term.

The paper is organized as follows. In Section 2 consider asymptotically safe gravity and look for the IR fixed point there. As a byproduct, we give a possible IR extension of the Nature-picked trajectory. In Section 3 we repeat the investigation for the conformally reduced quantum gravity. The evolution of the bilocal potential is treated in Section 4. Finally, in Section 5 the conclusions are drawn up.

2. Evolution Equations

First, we consider the standard local form of the asymptotically safe gravity. We look for the IR behavior of the model where the full metric is used as a path integral variable. For simplicity, we use the Wetterich equation [32]. It is based on considering the effective average action, where the macroscopic field variable is given by taking the average of the microscopic field variables on the volume with radius k^{-1}, where k plays the role of the RG cutoff scale. The effective average action Γ_k satisfies the Wetterich equation

$$\dot{\Gamma}_k = \frac{1}{2}\mathrm{Tr}\left(\dot{\mathrm{R}}_k[\Gamma^{(2)} + \mathrm{R}_k]^{-1}\right), \tag{1}$$

where the dot is ∂_t, with $t = \ln k$. We introduced the regulator R_k that changes rapidly at the cutoff resulting in a strong separation between low and high momentum modes. Usually, we use the Litim regulator

$$\mathrm{R}_k^{lit} = (k^2 - p^2)\theta(k^2 - p^2), \tag{2}$$

with the step function θ. It gives a contribution when the momentum of the mode is smaller than the cutoff, i.e., when $p^2 < k^2$. In the case of pure gravity without matter field, the effective average action can be given by the Einstein–Hilbert action

$$\Gamma_k = \frac{1}{16\pi G_k}\int_x \sqrt{g}(-R + 2\Lambda_k), \tag{3}$$

where $\sqrt{g} = \sqrt{\det(g)}$, with the metric g that is decomposed into background and fluctuating parts. Newton's constant G_k and the cosmological constant Λ_k become scale-dependent in the RG treatment. The Einstein–Hilbert action contains only these couplings, their dimensionless forms are $g_k = k^{d-2}G_k$ and $\lambda_k = k^{-2}\Lambda_k$. From now on their cutoff dependences are suppressed. The evolution equations using the Litim regulator are [9]

$$\begin{aligned} \dot{g} &= (2+\eta)g, \\ \dot{\lambda} &= -(2-\eta_N)\lambda + \frac{g}{8\pi}\left(\frac{20}{1-2\lambda} - 16 - \frac{10}{3}\eta\frac{1}{1-2\lambda}\right). \end{aligned} \tag{4}$$

The flow equation for Newton's constant is practically the definition of the anomalous dimension η. Its form can be given as

$$\eta = \frac{g(\frac{5}{1-2\lambda} - \frac{9}{(1-2\lambda)^2} - 7)}{3\pi(1 + \frac{g}{12\pi}(\frac{5}{1-2\lambda} - \frac{6}{(1-2\lambda)^2}))} \tag{5}$$

in $d = 4$. The model has two fixed points, a Gaussian fixed point (GFP), and a Reuter fixed point. The position of the fixed points are given in Table 1. We also listed the scaling exponents that describe the scaling properties of the couplings in the vicinity of the corresponding fixed points. They are the eigenvalues of the stability matrix, which comes from the linearized form of the flow equations at the fixed point. If they are negative, at least their real parts, then the fixed point is UV attractive. Mixed real values refer to hyperbolic fixed points.

Table 1. The position of the fixed points and the corresponding scaling exponents are presented for the Einstein–Hilbert action.

Fixed Point	g^*	λ^*	$s_{1,2}$
Gaussian	0	0	$-2; 2$
Reuter	0.707	0.193	$-1.48 \pm 3.04i$.

The central result of the asymptotically safe gravity is the UV attractive Reuter fixed point that makes the physical quantities finite. After solving the evolution equations numerically, the phase space can be mapped out, as can be seen in Figure 1.

The standard phase space shows that there is a UV-attractive Reuter fixed point and a hyperbolic GFP at the origin. The latter separates the two phases. The symmetric phase can correspond to the trajectories where the cosmological constant is negative in the IR. In the broken symmetric phase, the IR value of λ is positive, however, it cannot reach the $k \to 0$ limit.

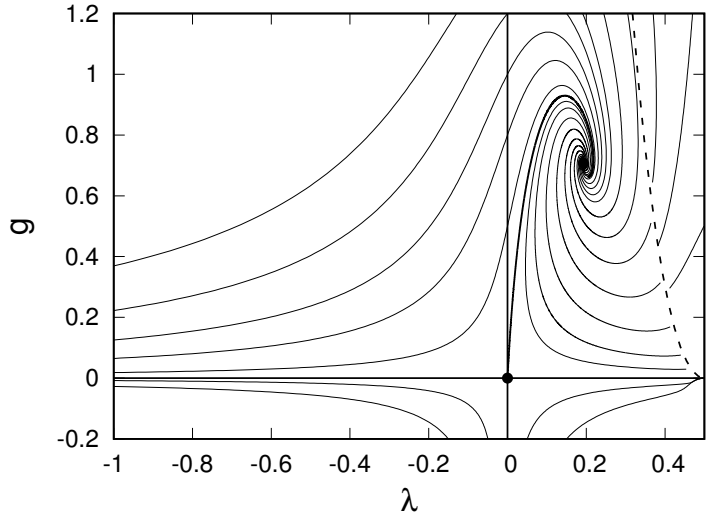

Figure 1. The phase space of the asymptotically safe gravity is presented in the g and λ plane. The dots show the Reuter and the Gaussian fixed points. The dashed curve denotes the points where the anomalous dimension η is singular. The figure is made based on [9].

2.1. Infrared Scaling

The singularity gives the IR limitation of the RG method in the broken symmetric phase. It suggests that the original degrees of freedom are not suitable anymore to describe the physical system, and presumably we should consider the quantum fluctuation around a nonlocal condensate [20,38]. The IR fixed point can be clearly identified in the phase diagram by realizing that the trajectories of the broken symmetric phase flow into an attractive point [39]. In the asymptotically safe gravity, the situation is a bit different, since in Figure 1 there is a line of singular points. It turns out that only a single point of the curve becomes the IR fixed point.

In order to obtain the IR fixed point analytically, we derive the transformed RG equations by changing the original couplings to new ones, where the evolution equations are not singular. There are two singularities in the flow equations, these define the new couplings, they are

$$\begin{aligned} \ell &= 1-2\lambda \\ y &= 12\pi(1-2\lambda)^2+(5(1-2\lambda)-6)g. \end{aligned} \tag{6}$$

The new coupling ℓ eliminates the singularity coming from the propagator. This is connected to the inverted action and the corresponding conformal factor instability. The coupling y is also connected to a singular behavior, it comes from the denominator of the anomalous dimension. We can derive evolution equations for ℓ and y and they are

$$\begin{aligned} \partial_\tau y &= -\frac{1}{12\pi(5\ell-6)}\big(5184\pi^3\ell^3(175\ell^5-300\ell^4+28\ell^3+173\ell^2-534\ell+216) \\ &\quad -72\pi^2\ell y(2800\ell^5-8405\ell^4+11559\ell^3-12900\ell^2+2124\ell+864) \\ &\quad +6\pi y^2(1750\ell^4-6455\ell^3+9271\ell^2-11958\ell+3816)+5y^3(10\ell+97)\big) \\ \partial_\tau \ell &= -6\pi(\ell-1)\ell^2+\frac{1}{2(5\ell-6)}\big((12\pi\ell^2-y)(((14\ell-43)\ell+47)\ell-12)\big) \\ &\quad -\frac{1}{12\pi(5\ell-6)^2}\big((12\pi\ell^2-y)^2(10\ell+97)\big). \end{aligned} \tag{7}$$

The singularity appears at finite scale k_{term} or t_{term}. The derivative should be also changed to push the scale k_{term} to zero, therefore, we introduce $\partial_\tau = y\partial_t$.

The IR fixed point appears in Table 2, it has zero scaling exponents; however, the flow shows that it is IR attractive.

Table 2. The position of the fixed points and the corresponding scaling exponents are presented for the transformed equation in Equation (7).

Fixed Point	y^*	ℓ^*	$s_{1,2}$
Gaussian	37.7	1	75.398; −18.85
Reuter	12.12	0.614	$-15.116 \pm i13.84$
IR	0	0	0; 0

2.2. Nature Picked Trajectory

The phase diagram in Figure 1 shows the paths for g and λ. At laboratory scales, the value of Newton's constant is known, it is

$$g(k_{lab}) = \left(\frac{l_{Pl}}{k_{lab}^{-1}}\right)^2 \approx 10^{-70}. \tag{8}$$

Here, we assumed that the laboratory scale is about 1 m. It may help us to identify which trajectory is realized by Nature [40]. The trajectory is quite unnatural in the sense that it is extremely close to the GFP. Since it is a hyperbolic point with one attracting and one repelling direction, the run on the trajectory slows down close to the GFP. It implies that the trajectory spends a lot of time near the GFP. The turning point k_T is situated approximately 30 orders of magnitude below the Planck scale. The scale of the IR singularity k_{term} is 30 magnitudes below k_T.

It is assumed that the trajectory belonging to Nature tends to an IR fixed point [40–43]. There the IR fixed point is interacting since g^* is nonzero. The IR fixed point of Equation (7) differs from the interacting IR fixed point because it can be found at the singularity points $g^* = 0$ and $\lambda^* = 1/2$; however, they are extremely close to each other. The IR fixed point belonging to the singularity condition can be considered as a noninteracting one. Both the interacting and the noninteracting IR fixed points are IR attractive; furthermore, they are reached at finite cutoff scale k_{term}. The significant difference comes from the fact, that the IR fixed point assumes an infinitesimally small g^*; therefore, the interacting IR fixed point is a non-Gaussian fixed point just like the UV Reuter fixed point. In contrast, the noninteracting IR fixed point is similar to the UV Lifshitz-type gravity fixed point where $g^* = 0$ with finite cosmological constant. The interacting IR fixed point needs $\eta = -2$, as in the case of the Reuter fixed point. In the general relativity regime η is practically zero, so it should change in a significant way in the IR regime. It needs a fundamental change in the g and λ dependence of η. The noninteracting fixed point does not require $\eta = -2$, so no significant change is needed, it can be realized in a smoother way.

It is assumed that new interactions can arise at low energy scales and can create the interacting IR fixed point. From a cosmological point of view, the cutoff is inversely proportional to the cosmological time t_c, i.e., $k \sim 1/t_c$, where the proportionality factor is around 1. Therefore, the vicinity of the interacting IR fixed point at low energies can correspond to large cosmological distances. We know that there is a deviation from classical cosmology at large distance scales, i.e., there is a discrepancy between the observable mass and the one obtained from observed motion for galactic systems. The standard IR behavior coming from the RG equations is based on the GFP scalings, and the regime of the general relativity can be derived from the GFP scaling of the flow equations [40]. The deviation from the general relativity, the classical cosmology, should be caused by new physics emerging at low energies; moreover, the possible new interaction can result in the interacting IR fixed point, too. We should note that there is no signal of the interacting IR fixed point in our treatment. According to our analysis, we can find only a noninteracting IR fixed point in the model. From now on we refer to it simply as the IR fixed point.

We can give a possible IR completion of Nature's picked trajectory. We can find the linearized solution of the flow equations in Equation (7) in the vicinity of the IR fixed point, and replacing the original couplings g and λ a cubic expression appears around the IR fixed point according to

$$g = \frac{53\pi}{9}(1-2\lambda)^3. \tag{9}$$

The general relativity regime can correspond to $g_T\lambda_T/2 = g\lambda$, implying that $g \approx g_T^2/\lambda$. Assuming that the flow is continuously differentiable we can join together the Gaussian and the IR scalings. The IR scale where the two functions are connected k_{IR} can be found at the deep IR regime. The cosmological constant at k_{IR} is

$$\lambda(k_{IR}) \approx \frac{1}{2} - g_T. \tag{10}$$

We could complete the Nature trajectory till the IR fixed point by joining the hyperbolic function of the Gaussian scaling with the third-order polynomial in the IR.

Our results show that the Einstein–Hilbert action in the present form does not seem to modify the IR behavior of the model. We expect that strong nonlocal interactions arise at low energy scales; however, the local theory cannot introduce such terms. At this point, it is worth noting that the local RG evolution is a simplification. It was shown that in the Wegner–Houghton equation there is a non-trivial saddle point in the eliminated modes of the momentum shell [44] and it gives a bilocal contribution to the evolution at the tree level. The bilocal contribution of the potential introduces a momentum-dependent coupling, which at small momenta can describe and can change large distance behavior.

Usually, the nonlocal evolution is dropped out. In the following sections, our goal is to find the evolution equation for the bilocal couplings and to see how it modifies the IR behavior.

3. Conformally Reduced Quantum Gravity

We can simplify the treatment by following only the conform factor of the metric. It is assumed that the metric constitutes a dynamical conformal factor and a non-dynamical reference metric $\hat{g}_{\mu\nu}$. The conformal factor is parameterized by a scalar field in such a way that it provides the traditional form of the kinetic term. We choose

$$g_{\mu\nu} = \phi^{2\nu(d)}\hat{g}_{\mu\nu} \tag{11}$$

with $\nu(d) = 2/(d-2)$ [45]. We can obtain the conformally reduced version of the Einstein–Hilbert action

$$S_{EH} = \frac{1}{8\pi\xi(d)G}\int d^4x\sqrt{\hat{g}}\left(\frac{1}{2}\hat{g}^{\mu\nu}\partial_\mu\phi\partial_\nu\phi + \frac{1}{2}\hat{R}\phi^2 - \xi(4d)\Lambda\phi^{2d/(d-2)}\right), \tag{12}$$

where $\hat{R}$ is the curvature of $\hat{g}_{\mu\nu}$; furthermore, $\xi(d) = (d-2)/(4(d-1))$ [20,22,46]. When $d = 4$, then $\nu = 1$, $\xi = 1/6$, $g_{\mu\nu} = \phi^2\hat{g}_{\mu\nu}$ and the Einstein–Hilbert action reduces to

$$S_{EH} = -\frac{3}{4\pi G}\int d^4x\sqrt{\hat{g}}\left(\frac{1}{2}\hat{g}^{\mu\nu}\partial_\mu\phi\partial_\nu\phi + \frac{1}{12}\hat{R}\phi^2 - \frac{1}{6}\Lambda\phi^4\right). \tag{13}$$

From now on we consider only the conformally reduced version of the action; therefore, we suppress the subscript, instead, we use the cutoff k. The microscopic field variable ϕ_x is split into the sum of the background field and the fluctuation, $\phi_x = \chi_B + \underline{f}_x$. It is assumed that the background field χ_B is constant. The blocked action is modified by a bilocal term with the bilocal coupling w_{xy}:

$$S_k = -Z_k \int_{xy} \sqrt{\hat{g}_x} \Big\{ \delta_{xy} \Big(-\frac{1}{2}(\chi_B + \underline{f}_x)\hat{\Box}(\chi_B + \underline{f}_x) + \frac{1}{12}\hat{R}(\chi_B + \underline{f}_x)^2 - \frac{\Lambda_k}{6}(\chi_B + \underline{f}_x)^4 \Big) - \frac{1}{4} w_{xy} (\chi_B + \underline{f}_x)^2 (\chi_B + \underline{f}_y)^2 \Big\}. \quad (14)$$

The Newton's constant G_k is contained in the wavefunction renormalization

$$Z_k = \frac{3}{4\pi G_k}. \quad (15)$$

We can introduce the compact notation of the local and the bilocal potentials

$$\begin{aligned} \mathcal{U}_k &= \frac{\Lambda_k}{6}\phi_x^4 - \frac{1}{12}\hat{R}\phi_x^2 \\ \mathcal{V}_k &= \frac{1}{4} W_{xy} \phi_x^2 \phi_y^2, \end{aligned} \quad (16)$$

after turning back to the variable ϕ_x. We assume the translational symmetry in the bilocal term, $W_{xy} = W_{x-y}$. The compact form of the conformally reduced Einstein–Hilbert action can be written as

$$S_k = -Z_k \int \sqrt{\hat{g}} \Big\{ \frac{1}{2}\phi(-\hat{\Box})\phi - \mathcal{U}_k - \mathcal{V}_k \Big\}. \quad (17)$$

The derivative of the action with respect to the cutoff gives

$$\frac{\dot{S}_k}{Z_k} = \int \Big(\eta \frac{1}{2} \underline{f}(-\hat{\Box})\underline{f} - \eta \mathcal{U}_k + \dot{\mathcal{U}}_k - \eta \mathcal{V} + \dot{\mathcal{V}}_k \Big), \quad (18)$$

where we have introduced the anomalous dimension

$$\eta = -\frac{\dot{Z}_k}{Z_k} = \frac{\dot{G}_k}{G_k}. \quad (19)$$

Without loss of generality, we can choose the flat reference metric $\hat{g}_{\mu\nu} = \delta_{\mu\nu}$ which implies that $\sqrt{\hat{g}} = 1$ and $\hat{\Box} = \Box$.

3.1. Evolution Equation

Since we intend to follow the evolution of the bilocal potential, we should use the Wegner–Houghton equation. There, the modes are split into UV and IR parts, i.e., $\phi \to \phi + \varphi$. The field variable ϕ belongs to modes characterized by the momentum in $k \in [0, k - \Delta k]$, while φ is with momentum in $k \in [k - \Delta k, k]$. The UV modes in the shell are integrated out, and it can correspond to an RG blocking step. The expression to be integrated is

$$e^{-S_{k-\Delta k}(\phi)} = \int D[\varphi] e^{-S_k[\phi+\varphi]} \approx \int D[\varphi] e^{-S_k[\phi+\varphi_0] - \frac{1}{2}\varphi \frac{\delta^2 S_k[\phi+\varphi_0]}{\delta\varphi\delta\varphi}\varphi}. \quad (20)$$

After the integration we obtain the Wegner–Houghton equation

$$\dot{S}_k[\phi] = -k\frac{S_k[\phi + \varphi_0] - S_k[\phi]}{\Delta k} - \frac{k}{2\Delta k} \mathrm{Tr} \ln \left[\frac{\delta^2 S_k[\phi + \varphi_0]}{\delta\phi\delta\phi} \right]. \quad (21)$$

The first term comes from the contribution of the non-trivial saddle point. This term is responsible for the nonlocal evolution. Considering only the local part of the evolution and using Equation (21) together with Equation (18) the evolution equation for the action is

$$\dot{S}_k[\phi] = -\frac{1}{2}\int_q \delta(k - |q|) \ln S_q'', \tag{22}$$

where S_q'' is the second derivative of the blocked action with respect to the field variable. The Dirac-delta restricts the momentum integration into an infinitesimally small thin momentum shell with radius k. After the integration we obtain

$$\dot{S}_k[\phi] = -\frac{1}{2}\alpha_d k^d \ln S_k'' \tag{23}$$

with

$$\alpha_d = \frac{\Omega_d}{(2\pi)^d}, \quad \Omega_d = \frac{2\pi^{d/2}}{\Gamma(d/2)}. \tag{24}$$

The renormalization treatment of the conformally reduced gravity can be performed in the framework of the Wegner–Houghton equation using Schwinger's proper-time regulator, too [25,47].

In the conformally reduced Einstein–Hilbert action the kinetic energy has an unusual negative sign. Nevertheless, the ϕ^4 term is positive definite; therefore, the action goes to infinity with growing ϕ. However, a rapid change in ϕ can make the action unbounded from below. This is the so-called conformal factor instability. The negative kinetic energy creates a kinetic condensate that is made from coordinate-dependent modes. A prominent example of a kinetic condensate is the gluon condensate in QCD, where the minimum is situated in the Savvidy vacuum with $F_{\mu\nu} \neq 0$; however, it turned out later, that this vacuum is IR unstable. Similar ideas were applied in quantum gravity models where the square of the curvature is included, guaranteeing the boundedness of the action [48,49]. The problem of kinetic condensate also appears in the Liouville field theory [50], where an inhomogeneous condensate may stabilize the vacuum. A similar inhomogeneous vacuum appears in spin systems in the case of antiferromagnetic order [51].

The other possibility to manage the instability problem is to use the so-called inverted action, $S_{inv} = -S$, that can be obtained by a proper choice of Wick rotation [20]. It makes the kinetic term positive at the price of changing the sign of the potential, too. This choice clearly gives an unstable action; however, it provides a physically relevant region where the calculation is acceptable. According to a naive geometrical picture, the double-well potential with two minima and a local maximum in the origin is inverted to its upside-down form, and we perform the calculation around the origin, which is now the minimum for the inverted action. The calculation is valid between the two maxima.

In the symmetric phase the evolution can reach the $k \to 0$ limit, there the cosmological constant is negative. However, due to the conform factor instability and the usage of the inverted action, there is a singularity in the broken symmetric phase. We expand the action around a local extremum; therefore, the reliability is guaranteed until $1 - 2\lambda > 0$. The instability in the broken symmetric phase usually turns up if we do not consider the quantum fluctuations around the running local minimum. In the ϕ^4 model, if we derive the evolution equations around the origin where the potential has a local maximum, the evolution runs into a singularity. Taking the evolution equations around the local minimum, we seemingly can avoid the singularity, however, it is not completely true. The singularity condition

$$k^2 + V'' = 0 \tag{25}$$

which typically appears in the dressed scalar propagators cannot be zero around a minimum, since $V'' > 0$. However, if a local minimum becomes a local maximum at a finite scale k, then we should jump the expansion point ϕ_0 from the old minimum to the new one. This cannot happen in a second-order phase transition, but in a first-order phase transition,

the change in the local minima is fundamental. It is also unphysical if the value ϕ_0 jumps from one local minimum to the other immediately as the new minimum value becomes absolute since they can be quite far from each other [52]. The singularity is also unavoidable in the 2-dimensional sine-Gordon modelI, where a Fourier expansion is used [53].

In the derivation of the Wegner–Houghton evolution equation, the renormalized propagator changes its sign, signaling the inverted action picture during the analysis. The inversion should be used in the case of the Wetterich equation, too. We can connect the two approaches of the evolution equations by a strange choice of the regulator [54]

$$R = R_0\theta(1 - p^2/k^2). \tag{26}$$

The regulator is zero if $k^2 < p^2 < \infty$, and nonzero for $p^2 < k^2$, where $R_0 \to \infty$. A very naive, mathematically superficial derivation might give

$$\dot{\Gamma} = \frac{1}{2}\mathrm{Tr}\frac{\dot{R}}{\Gamma'' + R} = \frac{1}{2}\alpha_d k^d \partial_k \int_{k^2}^{\infty} \ln \Gamma''. \tag{27}$$

Since the higher momentum modes contribute to the evolution, it suggests that the bare action and not the effective action evolves

$$\dot{S} = -\frac{1}{2}\alpha_d k^d \ln S'', \tag{28}$$

where we used the fact the derivation with respect to the cutoff acts only on the lower limit of the integral. Starting from the Wetterich equation we arrive at the Wegner–Houghton equation. A mathematically well-established derivation can be found in [54], where a Taylor expanded version of the potential is used, with well-defined integrals.

The derivation enlightens the similarity and the difference between the Wegner–Houghton and the Wetterich equations. The trace in the Wetterich equation is taken for the lower momenta according to the standard choices of the regulator. There, the average field plays the role of the average action that is nonzero for $0 < p^2 < k^2$ and it can be considered as a 'macroscopic' field variable. However, in the Wegner–Houghton equation, due to the special form of the regulator in Equation (26), the momentum integration is performed for high momenta. It implies that the original, microscopic field variables are taken into account, and they contribute to the evolution when their characteristic momenta satisfies $k^2 < p^2 < \infty$.

3.2. Infrared Scaling in Conformally Reduced Gravity

Keeping the $\mathcal{O}\left(\underline{f}^0\right)$ term in the Wegner–Houghton equation, and keeping only the local terms we obtain

$$-\eta U_k(\chi_B) + \dot{U}_k(\chi_B) = -\frac{1}{2}\frac{k^2\chi_B^2}{Z_k}\alpha_d \log\left(\chi_B^2 k^2 - 2\Lambda\chi_B^2 k^2 + \frac{1}{6}\hat{R}\right), \tag{29}$$

where the equation is normalized with the spacetime volume. After expanding in the curvature, we obtain the dimensionless evolution equations

$$\begin{aligned} \dot{\lambda} &= -(2-\eta)\lambda - \frac{g}{2\pi}\ln(1-2\lambda) \\ \dot{g} &= (2+\eta)g \\ \eta &= -\frac{g}{6\pi}\frac{1}{1-2\lambda}, \end{aligned} \tag{30}$$

where the anomalous dimension is obtained from the linear term in the Ricci scalar $\hat{R}$. The fixed points of the model can be found in Table 3. They are the standard ones, the Gaussian and the Reuter fixed points, the latter has complex scaling exponents.

Table 3. The position of the fixed points and the corresponding scaling exponents for conformally reduced gravity are given, where the anomalous dimension is calculated from the potential term.

Fixed Point	g^*	λ^*	$s_{1,2}$
Gaussian	0	0	$2; -2$
Reuter	5.617	0.426	$-2.711 \pm i4.726$

The RG equations show singular behavior. It can be eliminated by transforming the coupling λ according to

$$\ell = -\frac{1}{\ln(1-2\lambda)}. \tag{31}$$

The choice gives finite value in the IR fixed point, i.e., if $\lambda \to 1/2$ then $\ell \to 0$. The GFP can be found at the $\ell \to \infty$ limit. Although the infinite value of any couplings is unphysical, it does not cause any problem at the GFP, since it is a hyperbolic point, therefore, it cannot be reached by the trajectories. The coupling g is kept unchanged. The evolution of ℓ reads as

$$\dot{\ell} = -2\lambda e^{1/\ell}\ell^2, \tag{32}$$

and the transformed flow equations become

$$\begin{aligned} \partial_\tau g &= 2e^{-2/\ell}g - \frac{e^{-1/\ell}g^2}{6\pi} \\ \partial_\tau \ell &= 2e^{-1/\ell}\ell^2\left(1-e^{-1/\ell}\right) + \frac{1}{6\pi}\left(g\ell^2 - e^{-1/\ell}\ell g(6+\ell)\right), \end{aligned} \tag{33}$$

with $\partial_\tau = e^{-2/\ell}\partial_t$. The fixed points are collected in Table 4.

Table 4. The position of the fixed points and the corresponding scaling exponents for conformally reduced gravity are given after the transformation of λ to ℓ, where the anomalous dimension is calculated from the potential term.

Fixed Point	g^*	ℓ^*	$s_{1,2}$
Gaussian	0	∞	$2; 2$
Reuter	5.617	0.525	$-0.06 \pm i0.1$
IR	0	0	$0; 0$

It says that the GFP has two repelling directions, since due to the definition of the new coupling ℓ, it becomes irrelevant around the GFP. The Reuter fixed point has complex scaling exponents. We can find an IR fixed point, it is IR attractive; however, the scaling exponents are zero.

A similar procedure can be used when η comes from the kinetic term [20]. The flow equations become

$$\begin{aligned} \dot{\lambda} &= -(2-\eta)\lambda - \frac{g}{2\pi}\ln(1-2\lambda) \\ \dot{g} &= (2+\eta)g \\ \eta &= -\frac{8g\lambda^3}{4\pi}\frac{1}{(1-2\lambda)^4}. \end{aligned} \tag{34}$$

The fixed points are given in Table 5, containing the Gaussian and the Reuter fixed points.

Table 5. The position of the fixed points and the corresponding scaling exponents for conformally reduced gravity are shown, where the anomalous dimension is calculated from the kinetic term.

Fixed Point	g^*	λ^*	$s_{1,2}$
Gaussian	0	0	$2; -2$
Reuter	6.793	0.375	$-4.069 \pm i4.163$

We can use the transformation of λ according to Equation (32) in this case, too, and it gives

$$\begin{aligned} \partial_\tau g &= 2e^{-5/\ell} g + \frac{16 e^{-1/\ell} g^2}{3\pi(1+e^{1/\ell})^4}\left(e^{-1/\ell}-1\right)^3 \\ \partial_\tau \ell &= e^{-4/\ell}\ell\left(-2\ell e^{-1/\ell} + 2\ell - \frac{g}{\pi}\right) + \frac{16 g \ell^2}{3\pi(1+e^{1/\ell})^4}\left(e^{-1/\ell}-1\right)^4, \end{aligned} \tag{35}$$

with $\partial_\tau = e^{-5/\ell}\partial_t$. Again, the GFP has two repulsive directions, and the Reuter fixed point has complex scaling exponents, they are given in Table 6. The IR fixed point also appears, with an IR attractive nature.

Table 6. The position of the fixed points and the corresponding scaling exponents for conformally reduced gravity are presented after the transformation of λ to ℓ, where the anomalous dimension is calculated from the kinetic term.

Fixed Point	g^*	ℓ^*	$s_{1,2}$
Gaussian	0	∞	$2; 2$
Reuter	6.793	0.72	$-0.0039 \pm i0.004$
IR	0	0	$0; 0$

4. Bilocal Evolution

The local evolution enables us to give an IR completion of the trajectories. Using several calculation schemes, we obtained that there is an IR attractive IR fixed point. Next, we consider how the nonlocal effects can change the IR behavior.

Expansion around a Homogeneous Background

We decompose a general action for scalar field theory containing a bilocal term as

$$S_k = \frac{1}{2}\int_x \underline{\mathrm{f}}_x D_B^{-1} \underline{\mathrm{f}}_x + \int_x \tilde{U}(\chi_B + \underline{\mathrm{f}}_x) + \int_{xy} \tilde{V}_{x-y}(\chi_B + \underline{\mathrm{f}}_x, \chi_B + \underline{\mathrm{f}}_y). \tag{36}$$

In order to obtain the proper local limit of the potential, another decomposition is necessary according to

$$S_k = \Omega U_0(\chi_B) + \frac{1}{2}\int_x \underline{\mathrm{f}}_x D_B^{-1} \underline{\mathrm{f}}_x + \int_x U(\underline{\mathrm{f}}_x) + \int_{xy} V_{x-y}(\underline{\mathrm{f}}_x, \underline{\mathrm{f}}_y), \tag{37}$$

with the general local term

$$U_0(\chi_B) = \tilde{U}(\chi_B) + \tilde{V}_0(\chi_B, \chi_B). \tag{38}$$

The local and the bilocal decompositions have the form

$$\begin{aligned}\int_x U(f_x) &= \int_x [\tilde{U}(\chi_B + \underline{f}_x) - \tilde{U}(\chi_B) \\ &\quad + \tilde{V}_0(\chi_B + \underline{f}_x, \chi_B) + \tilde{V}_0(\chi_B, \chi_B + \underline{f}_x) - 2\tilde{V}_0(\chi_B, \chi_B)] \\ \int_{xy} V_{x-y}(\underline{f}_1, \underline{f}_2) &= \int_{xy} [\tilde{V}_{x-y}(\chi_B + \underline{f}_x, \chi_B + \underline{f}_y) \\ &\quad - \tilde{V}_{x-y}(\chi_B, \chi_B + \underline{f}_y) - \tilde{V}_{x-y}(\chi_B + \underline{f}_x, \chi_B) + \tilde{V}_{x-y}(\chi_B, \chi_B)], \end{aligned} \quad (39)$$

respectively. They clearly show that the local and bilocal terms mix with each other. The second derivative of the action is

$$S''_{xy}[\underline{f}] = D^{-1}_{xy} - \Sigma_{xy}[\underline{f}], \quad (40)$$

where the self-energy is

$$\begin{aligned}\Sigma_{xy}[\underline{f}] &= -\delta_{xy} U''(\underline{f}_x) - 2\partial_1\partial_2 V_{x-y}(\underline{f}_x, \underline{f}_y) - \delta_{xy} \int_z [\partial_1^2 V_{x-z}(\underline{f}_x, \underline{f}_z) + \partial_2^2 V_{z-x}(\underline{f}_z, \underline{f}_x)] \\ &\quad + \delta_{xy} U''(0) + 2\partial_1\partial_2 V_{x-y}(0,0) + \delta_{xy} \int_z [\partial_1^2 V_{x-z}(0,0) + \partial_2^2 V_{z-x}(0,0)], \end{aligned} \quad (41)$$

and D^{-1}_{xy} is the dressed propagator. Using the concrete forms of the potentials from Equation (16) we obtain

$$\Sigma_{xy}[\underline{f}] = -2\Lambda_k \underline{f}_x^2 - 4\chi_B \Lambda_k \underline{f}_x - W_0 \underline{f}_x^2 - 2\chi_B W_0 \underline{f}_x - 2W_{x-y} \underline{f}_x \underline{f}_y, \quad (42)$$

where the last term is bilocal. After the Fourier transformation, it becomes momentum-dependent coupling, $W_{x-y} \to W_q$. The bilocal coupling also appears in the local part of the self-energy in the form of the zero mode $W_{q=0} = W_0$. The propagator in momentum space can be written as

$$D_q^{-1} = -q^2 + K_q + m^2, \quad (43)$$

with $m^2 = 2\Lambda_k \chi_B^2 + W_0 \chi_B^2$ and $K_q = 2W_q \chi_B^2$. After reparameterization by Z_k and using the inverted conformally reduced Einstein–Hilbert action, the propagator becomes

$$D^{-1} = Z_k(q^2 - 2\Lambda_k \chi_B^2 - W_0 \chi_B^2 - 2W_q \chi_B^2). \quad (44)$$

We can obtain the evolution equation for λ by taking the $\mathcal{O}\left(\underline{f}^0\right)$ terms from the derivative of the action

$$\begin{aligned}\dot{S}_k &= -Z_k \int_x \left(-\frac{1}{12}\eta \hat{R} \chi_B^2 - \frac{1}{6}(\dot{\Lambda}_k - \Lambda_k \eta)\chi_B^4 - \frac{1}{4}(\dot{W}_0 - W_0 \eta)\chi_B^4 \right) \\ &\quad - Z_k \int_{xy} \left(-\frac{1}{2}\underline{f}_x \delta_{xy} \eta (-\hat{\Box}_y) \underline{f}_y - \frac{1}{4}\chi_B^2 \underline{f}_x (\dot{W}_{x-y} - W_{x-y}\eta) \underline{f}_y \right). \end{aligned} \quad (45)$$

It contains a constant and a linear term in $\hat{R}$. The former provides the flow equation for λ and the latter can give η as in the local case. The $\mathcal{O}\left(\underline{f}^2\right)$ terms contribute to the bilocal evolution, it is

$$\dot{w}_q = (-2 + \eta) w_q - \frac{4k}{Z_k} \int_p D^{(k)}_{p+q} w_p, \quad (46)$$

where the dimensionless bilocal coupling was introduced, $w_q = k^{-2} W_q$. We follow only the zero mode w_0 in the calculations, where the integral on the r.h.s. can be analytically performed. The zero mode starts to evolve since the integral picks up the contribution from the tree level evolution of w_k [44]. The evolution equations including the zero mode are

$$\begin{aligned}
\dot{g} &= (2+\eta)g \\
\dot{\lambda} &= (-2+\eta)\lambda + \frac{3}{2}(\eta w_0 - \dot{w}_0) - \frac{g}{2\pi}\ln(1-2\lambda-w_0-2w_k) \\
\dot{w}_0 &= (-2+\eta)w_0 - \frac{2g}{3\pi}\frac{1}{1-2\lambda-w_0-2w_k}w_k \\
\eta &= -\frac{g}{6\pi}\frac{1}{1-2\lambda-w_0-2w_k} \\
w_k &= -2\frac{\lambda^2}{1-2\lambda-w_0}.
\end{aligned} \tag{47}$$

Besides the standard couplings of the Einstein–Hilbert action g and λ, the zero mode w_0 appears as a new coupling. We note that the tree-level value of w_k is nonzero, therefore, it initiates the zero mode evolution. The flow equations have two fixed points, they are listed in Table 7.

Table 7. The position of the fixed points and the corresponding scaling exponents are shown for conformally reduced gravity with bilocal interaction.

Fixed Point	g^*	l^*	w_0^*	$s_{1,2,3}$
Gaussian	0	0	0	$-2;-2;2$
Reuter	25.141	0.167	0.318	$-47.25;-2.08;-0.45$

The Reuter fixed point is UV attractive with three negative real scaling exponents. The zero mode coupling proves to be relevant throughout its whole evolution. The new singularity relation

$$1-2\lambda-w_0=0 \tag{48}$$

also contains the zero mode. The l.h.s. should be greater than zero during the evolution. The GFP is a hyperbolic point, w_0 is relevant there. We sketched the phase diagram in Figure 2.

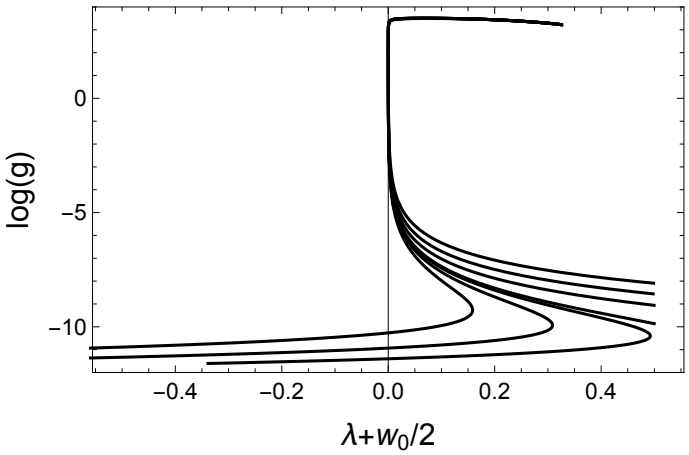

Figure 2. The phase space of asymptotically safe gravity is presented in the g and $\lambda + w_0/2$ plane. We set $w_0(t_i) = 0.001$, $g(t_i) = 0.01$, and $\lambda(t_i) = 0.008; 0.009; 0.0097; 0.01; 0.012; 0.015; 0.02$.

Although the zero mode starts to evolve due to the tree-level contribution even if its bare value is zero, the phase structure can be drawn by choosing arbitrary bare values. The bare couplings appearing in the action correspond to the values where the evolution starts. In quantum gravity, they can be chosen close to the Reuter fixed point, and this choice can be motivated mostly since the higher energy could mean smaller distances,

and then the flows pick up most information about the microscopic behavior of the model. The RG method can map the phase structure of the model, but the correspondence between the bare couplings and observables is very difficult. A possible approach can be to identify the bare couplings to the laboratory values. In this case, they are situated in a Nature-picked trajectory, very close to the GFP.

The phase space is three-dimensional, we plotted how g depends on $\lambda + w_0/2$. We choose logarithmic scaling for g since it shows the infrared behavior more. The trajectories start from the vicinity of the Reuter fixed point and approach the origin of the phase space; they can go arbitrarily close to the GFP. There are trajectories that run into instability, they belong to the broken symmetric phase and terminate at a finite scale t_{term}. The trajectories belonging to the symmetric phase tend to have negative values of λ. From Figure 2 we can see, that there is a significant difference if we compare the bilocal phase structure to the traditional local one in Figure 1. The discrepancy comes from the trajectories of the symmetric phase. The new bilocal phase space contains such trajectories where they seem to approach the singularity; however, the beta function of the cosmological constant changes its sign, and λ starts to decrease and then it continues its flow to negative infinity. These types of trajectories are missing in local evolutions where the separation of the phase is located around the GFP. In the bilocal evolution, it seems to happen around the instability region in the vicinity of the IR fixed point. The qualitative behavior appearing in Figure 2 is typical for the bilocal treatment, insensitive to the initial values of the couplings. The value of g remains positive during the evolution, its value monotonically decreases in the IR limit.

The bilocal phase space structure suggests that the IR fixed point is not an IR attractive point anymore, but a hyperbolic point. The reason is that the zero mode keeps its relevance throughout its flow, and makes the IR fixed point a hyperbolic one. It is interesting to notice that the symmetric phase contains two types of trajectories. One type is the standard flow, which turns to negative λ at the GFP. The other type of flow approaches the IR fixed point and then tends to negative λ. The flows with an infinitesimal difference in their bare values give infinitesimal change in the IR; therefore, they belong to the same phase. However, the latter flows have information on the IR fixed point, the former ones do not. The trajectory chosen by Nature can also belong to the latter type of trajectory.

We plotted the scale dependence of couplings in Figures 3 and 4.

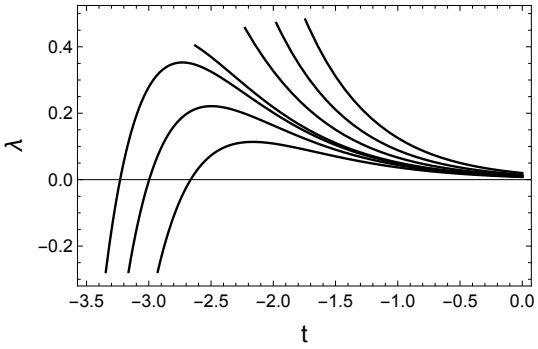

Figure 3. The cosmological constant is plotted for the initial condition used in Figure 2. When the evolution stops, then the flow runs into singularity (broken symmetric phase). The rest flows turn to negative values (symmetric phase).

The zero mode could change the beta function of λ in such a way, that it changes its sign, and it turns back the evolution of λ into the negative values. The other couplings scale monotonically. Although the value of g is very small, it is not zero; therefore, it seems, that there is no interacting IR fixed point in the bilocal model.

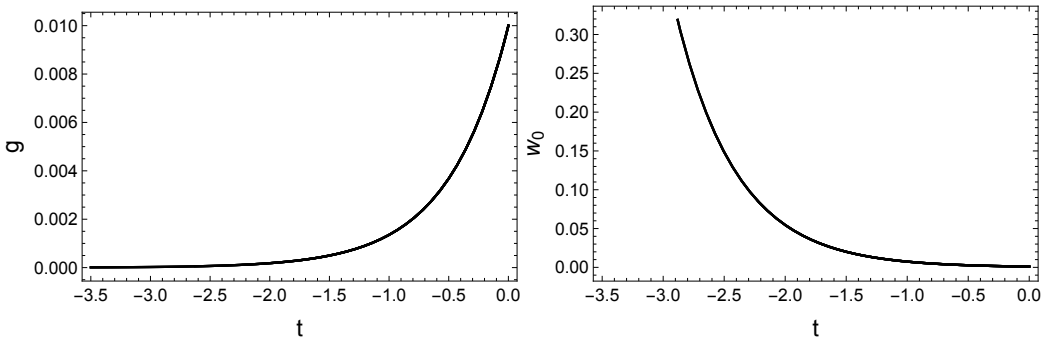

Figure 4. The Newton's constant and the zero modes are plotted using the initial condition used in Figure 2. The former always goes to zero, while the latter always grows up.

The evolution of couplings is slow in the vicinity of the GFP, and they speed up close to the IR fixed point. In this sense, the IR fixed point is not a classical hyperbolic point, where the slowing down of the flow appears, e.g., in the case of the Wilson–Fisher fixed point. The IR fixed point has zero scaling exponents, its hyperbolic nature can be demonstrated only by the numerical scaling behavior. The missing of the slowing down can be revealed in the flow of the cosmological constant in Figure 3. Thus, although the symmetric phase trajectories can be arbitrarily close to the singularity, they do not spend too much time there. It can also be demonstrated by plotting the singularity condition in Equation (48), as can be seen in Figure 5.

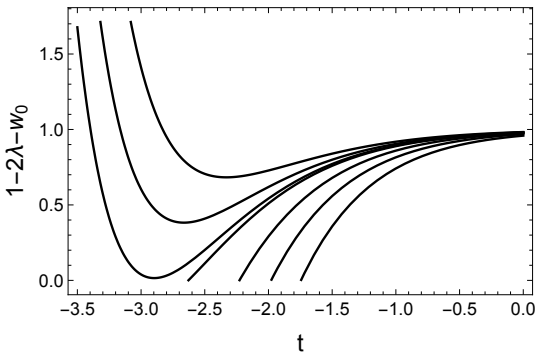

Figure 5. The expression in the singularity condition in Equation (48) is plotted for various initial condition used in Figure 2. The zero value is reached in the broken symmetric phase, but the trajectories of the symmetric phase can arbitrarily approach the zero value.

It is clear that the IR behavior of the bilocal model is even more important than in the local case; therefore, it is worth finding the IR fixed point by a proper transformation. The bilocal flow equations have similar singularities as the locals had, so similarly to Equation (31) we introduce the new variable

$$\ell = -\frac{1}{\ln(1-2\lambda-w_0)}. \tag{49}$$

The IR fixed point can be found at $\lambda + w_0/2 \to 1/2$ where $\ell \to 0$. Again, the GFP can be found at the $\ell \to \infty$ limit. The evolution of the new coupling comes from the relation

$$\dot{\ell} = -(\dot{w}_0 + 2\dot{\lambda})e^{1/\ell}\ell^2. \tag{50}$$

The evolution equations with the new coupling become

$$
\begin{aligned}
\partial_\tau g &= 2ge^{-1/\ell} - \frac{g^2 d_\ell}{6\pi} \\
\partial_\tau \ell &= \Big(\ell\big(-12\pi\ell(2+e^{3/\ell}(w_0-1)^2(3w_0-1)+4e^{1/\ell}(2w_0-1)+e^{2/\ell}(7w_0^2-10w_0+3)\big) \\
&\quad + ge^{1/\ell}(3(\ell+4)+2e^{2/\ell}(2\ell+3)(w_0-1)^2+e^{1/\ell}(12(w_0-1)+\ell(8w_0-7))) \\
&\quad + 6g\ell e^{1/\ell}(2+2e^{1/\ell}(w_0-1)+e^{2/\ell}(w_0-1)^2)\log(e^{2/\ell}d_\ell^{-1})\Big)\frac{d_\ell e^{-1/\ell}}{6\pi} \\
\partial_\tau w_0 &= -2w_0 e^{-1/\ell} - \frac{g(2e^{-1/\ell}+(3w_0-4)+2(w_0-1)^2e^{1/\ell})d_\ell}{6\pi},
\end{aligned}
\tag{51}
$$

where we introduced

$$
d_\ell^{-1} = 1 + (1+(w_0-1)e^{1/\ell})^2 \tag{52}
$$

and $\partial_\tau = e^{-2/\ell}\partial_t$. The fixed points are listed in Table 8.

Table 8. The position of the fixed points and the corresponding scaling exponents for conformally reduced gravity with bilocal interaction are shown after the transformation of λ to ℓ.

Fixed Point	g^*	ℓ^*	w_0^*	$s_{1,2,3}$
Gaussian	0	∞	0	$-2; 2; 2$
Reuter	25.141	0.949	0.318	$-19.64; -0.7; -0.34$
IR	0	0	$[0; 1/4]$	$0; 0; 0$

We can find three fixed points, the Reuter fixed point with three negative real exponents, the hyperbolic GFP, and the IR fixed point, where all the scaling exponents are zero. Again, ℓ becomes irrelevant, therefore, its exponent is positive in the GFP; however, w_0 remains relevant there. It implies that the zero mode provides a perturbatively renormalizable coupling.

Compared to the local model, in the bilocal case, the position of the IR fixed point can vary with the initial conditions. Similar to the previous situations, ℓ^* is always zero in the IR fixed point, but the zero mode value w_0^* can change. The IR fixed point of the local case can naturally correspond to $w_0^* = 0$. However, w_0^* cannot be larger than $1/4$ otherwise we cannot satisfy the relation coming from Equation (48). From ℓ we can calculate the IR fixed point value of the cosmological constant, it gives $\lambda^* = (1 - w_0^*)/2$, so it can vary in the interval $[3/8; 1/2]$.

This IR fixed point corresponds to $g^* = 0$, therefore, it is not an interacting IR fixed point. One can conclude that the nonlocality of the model cannot find an interacting fixed point, but it can change the monotonic tendency of the λ flow. The hyperbolic nature of the IR fixed point can raise an important question: where is Nature's picked trajectory? Since we cannot associate a bare zero mode value to the flow chosen by Nature, we can suppose that our trajectory runs into the singularity, as we assumed so far; however, it can turn back and can run into negative values of λ. It may imply that the sign of the cosmological constant changes in the deep IR evolution and becomes negative.

5. Summary

The infrared behavior of the asymptotically safe gravity has been investigated in the framework of the functional renormalization group method. We found an infrared fixed point of the model, both in the original and in the conformally reduced version of gravity. We showed that the infrared fixed point has zero scaling exponents; nevertheless, the scaling behaviors show that the fixed point is attractive.

Letting the bilocal evolution evolve, we were able to complete the traditional evolution equations with the evolution of the zero mode. It changed the IR behavior of the model

in such a way that the attractive IR fixed point became a hyperbolic one, consequently the cosmological constant flow is not necessarily monotonic. It can raise the question of whether Nature's picked trajectory remains in the broken symmetric phase or moves to the symmetric phase, characterized by negative cosmological constants.

We should emphasize that our investigation is not a possible extension of the asymptotically safe gravity with a bilocal coupling. We argue that the RG blocking step generates bilocal terms into the potential, which should be taken into account since it gives tree-level contribution to the evolution; therefore, there is no reason to leave them out from the RG treatment. It seems that the local approach of the RG method is incomplete, and taking into account nonlocal interaction is a necessary way to improve the calculations. It is proven by the results that due to the bilocal evolution, the IR physics of the asymptotically safe gravity changes fundamentally. In the foregoing work we intend to study the nonlocal effects in the original model of the asymptotically safe gravity.

Funding: This research received no external funding.

Data Availability Statement: The datasets generated and analyzed during the current study are available from the corresponding author upon reasonable request.

Conflicts of Interest: The author declares no conflicts of interest.

References

1. Berges, J.; Tetradis, N.; Wetterich, C. Nonperturbative renormalization flow in quantum field theory and statistical physics. *Phys. Rep.* **2002**, *363*, 223–386. [CrossRef]
2. Dupuis, N.; Canet, L.; Eichhorn, A.; Metzner, W.; Pawlowski, J.M.; Tissier, M.; Wschebor, N. The nonperturbative functional renormalization group and its applications. *Phys. Rep.* **2021**, *910*, 1–114.
3. Gies, H. Introduction to the functional RG and applications to gauge theories. *Lect. Notes Phys.* **2012**, *852*, 287–348.
4. Morris, T.R. The Exact renormalization group and approximate solutions. *Int. J. Mod. Phys.* **1994**, *A9*, 2411–2450. [CrossRef]
5. Pawlowski, J.M. Aspects of the functional renormalisation group. *Ann. Phys.* **2007**, *322*, 2831–2915. [CrossRef]
6. Polonyi, J. Lectures on the functional renormalization group method. *Cent. Eur. J. Phys.* **2003**, *1*, 1–71. [CrossRef]
7. Wilson, K.G. Renormalization group and critical phenomena. 1. Renormalization group and the Kadanoff scaling picture. *Phys. Rev.* **1971**, *B4*, 3174–3183. [CrossRef]
8. Bonanno, A.; Eichhorn, A.; Gies, H.; Pawlowski, J.M.; Percacci, R.; Reuter, M.; Saueressig, F.; Vacca, G.P. Critical reflections on asymptotically safe gravity. *Front. Phys.* **2020**, *8*, 269. [CrossRef]
9. Saueressig, F. The Functional Renormalization Group in Quantum Gravity. *arXiv* **2023**, arXiv:2302.14152.
10. Reuter, M.; Saueressig, F. *Quantum Gravity and the Functional Renormalization Group: The Road towards Asymptotic Safety*; Cambridge University Press: Cambridge, UK, 2019; p. 1.
11. Eichhorn, A. An asymptotically safe guide to quantum gravity and matter. *Front. Astron. Space Sci.* **2019**, *5*, 47. [CrossRef]
12. Pawlowski, J.M.; Reichert, M. Quantum Gravity: A Fluctuating Point of View. *Front. Phys.* **2021**, *8*, 551848. [CrossRef]
13. Percacci, R. *An Introduction to Covariant Quantum Gravity and Asymptotic Safety, 100 Years of General Relativity*; World Scientific: Singapore, 2017; Volume 3.
14. Reuter, M. Nonperturbative evolution equation for quantum gravity. *Phys. Rev.* **1998**, *D57*, 971–985. [CrossRef]
15. Laiho, J.; Bassler, S.; Coumbe, D.; Du, D.; Neelakanta, J.T. Lattice Quantum Gravity and Asymptotic Safety. *Phys. Rev. D* **2017**, *96*, 064015. [CrossRef]
16. Loll, R. Quantum Gravity from Causal Dynamical Triangulations: A Review. *Class. Quantum Gravity* **2020**, *37*, 013002. [CrossRef]
17. Hamber, H.W. Scaling Exponents for Lattice Quantum Gravity in Four Dimensions. *Phys. Rev. D* **2015**, *92*, 064017. [CrossRef]
18. Eichhorn, A.; Koslowski, T.; Pereira, A.D. Status of background-independent coarse-graining in tensor models for quantum gravity. *Universe* **2019**, *5*, 53. [CrossRef]
19. Gubitosi, G.; Ooijer, R.; Ripken, C.; Saueressig, F. Consistent early and late time cosmology from the RG flow of gravity. *JCAP* **2018**, *12*, 004. [CrossRef]
20. Reuter, M.; Weyer, H. Background Independence and Asymptotic Safety in Conformally Reduced Gravity. *Phys. Rev.* **2009**, *D79*, 105005. [CrossRef]
21. Gubitosi, G.; Ripken, C.; Saueressig, F. Scales and hierachies in asymptotically safe quantum gravity: A review. *Found. Phys.* **2019**, *49*, 972–990. [CrossRef]
22. Reuter, M.; Weyer, H. The Role of Background Independence for Asymptotic Safety in Quantum Einstein Gravity. *Gen. Relativ. Gravit.* **2009**, *41*, 983–1011. [CrossRef]
23. Nagy, S.; Polonyi, J.; Steib, I. Quantum renormalization group. *Phys. Rev.* **2016**, *D93*, 025008. [CrossRef]
24. Wegner, F.J.; Houghton, A. Renormalization group equation for critical phenomena. *Phys. Rev.* **1973**, *A8*, 401–412. [CrossRef]
25. Bonanno, A.; Reuter, M. Proper time flow equation for gravity. *JHEP* **2005**, *2*, 035. [CrossRef]

26. Codello, A.; Percacci, R.; Rahmede, C. Investigating the Ultraviolet Properties of Gravity with a Wilsonian Renormalization Group Equation. *Ann. Phys.* **2009**, *324*, 414–469. [CrossRef]
27. Manrique, E.; Reuter, M. Bare Action and Regularized Functional Integral of Asymptotically Safe Quantum Gravity. *Phys. Rev. D* **2009**, *79*, 025008. [CrossRef]
28. Nagy, S.; Sailer, K. Interplay of fixed points in scalar models. *Int. J. Mod. Phys.* **2013**, *A28*, 1350130. [CrossRef]
29. Braun, J.; Gies, H.; Scherer, D.D. Asymptotic safety: A simple example. *Phys. Rev.* **2011**, *D83*, 085012. [CrossRef]
30. Nagy, S.; Krizsan, J.; Sailer, K. Infrared fixed point in quantum Einstein gravity. *JHEP* **2012**, *1207*, 102. [CrossRef]
31. Christiansen, N.; Litim, D.F.; Pawlowski, J.M.; Rodigast, A. Fixed points and infrared completion of quantum gravity. *Phys. Lett. B* **2014**, *728*, 114–117. [CrossRef]
32. Wetterich, C. Exact evolution equation for the effective potential. *Phys. Lett.* **1993**, *B301*, 90–94. [CrossRef]
33. Bonanno, A.M.; Conti, M.; Cacciatori, S.L. Ultraviolet behavior of conformally reduced quadratic gravity. *Phys. Rev. D* **2023**, *108*, 026008. [CrossRef]
34. Machado, P.F.; Percacci, R. Conformally reduced quantum gravity revisited. *Phys. Rev. D* **2009**, *80*, 024020. [CrossRef]
35. Knorr, B. Lessons from conformally reduced quantum gravity. *Class. Quantum Gravity* **2021**, *38*, 065003. [CrossRef]
36. Buchbinder, I.L.; Odintsov, S.D.; Shapiro, I.L. *Effective Action in Quantum Gravity*; IOP Publishing Ltd.: Bristol, UK, 1992.
37. Falkenberg, S.; Odintsov, S.D. Gauge dependence of the effective average action in Einstein gravity. In Proceedings of the 8th Marcel Grossmann Meeting on Recent Developments in Theoretical and Experimental General Relativity, Gravitation, and Relativistic Field Theories, (MG 8), Jerusalem, Israel, 22–27 June 1997; Volume 6, pp. 800–802.
38. Alexandre, J.; Branchina, V.; Polonyi, J. Instability induced renormalization. *Phys. Lett.* **1999**, *B445*, 351–356. [CrossRef]
39. Nagy, S. Lectures on renormalization and asymptotic safety. *Ann. Phys.* **2014**, *350*, 310–346. [CrossRef]
40. Reuter, M.; Weyer, H. Quantum gravity at astrophysical distances? *JCAP* **2004**, *12*, 001. [CrossRef]
41. Bentivegna, E.; Bonanno, A.; Reuter, M. Confronting the IR fixed point cosmology with high redshift supernova data. *JCAP* **2004**, *01*, 001.
42. Bonanno, A.; Reuter, M. Cosmological perturbations in renormalization group derived cosmologies. *Int. J. Mod. Phys. D* **2004**, *13*, 107–122. [CrossRef]
43. Reuter, M.; Weyer, H. Running Newton constant, improved gravitational actions, and galaxy rotation curves. *Phys. Rev. D* **2004**, *70*, 124028. [CrossRef]
44. Nagy, S.; Polonyi, J.; Steib, I. Euclidean scalar field theory in the bilocal approximation. *Phys. Rev.* **2018**, *D97*, 085002. [CrossRef]
45. Jackiw, R.; Nunez, C.; Pi, S.Y. Quantum relaxation of the cosmological constant. *Phys. Lett. A* **2005**, *347*, 47–50. [CrossRef]
46. Reuter, M.; Weyer, H. Conformal sector of Quantum Einstein Gravity in the local potential approximation: Non-Gaussian fixed point and a phase of unbroken diffeomorphism invariance. *Phys. Rev. D* **2009**, *80*, 025001. [CrossRef]
47. Bonanno, A.; Lacagnina, G. Spontaneous symmetry breaking and proper time flow equations. *Nucl. Phys. B* **2004**, *693*, 36–50. [CrossRef]
48. Bonanno, A.; Reuter, M. Modulated Ground State of Gravity Theories with Stabilized Conformal Factor. *Phys. Rev.* **2013**, *D87*, 084019. [CrossRef]
49. Lauscher, O.; Reuter, M.; Wetterich, C. Rotation symmetry breaking condensate in a scalar theory. *Phys. Rev. D* **2000**, *62*, 125021. [CrossRef]
50. D'Hoker, E.; Jackiw, R. Space translation breaking and compactification in the liouville theory. *Phys. Rev. Lett.* **1983**, *50*, 1719–1722. [CrossRef]
51. Kojima, K.M.; Fudamoto, Y.; Larkin, M.; Luke, G.M.; Merrin, J.; Nachumi, B.; Uemura, Y.J.; Hase, M.; Sasago, Y.; Uchinokura, K.; et al. Antiferromagnetic order with spatially inhomogeneous ordered moment size of zn- and si-doped cugeo$_3$. *Phys. Rev. Lett.* **1997**, *79*, 503–506. [CrossRef]
52. Nagy, S.; Polonyi, J. First order phase transition with functional renormalization group method. *arXiv* **2024**, arXiv:2405.11043.
53. Nagy, S.; Nandori, I.; Polonyi, J.; Sailer, K. Functional renormalization group approach to the sine-Gordon model. *Phys. Rev. Lett.* **2009**, *102*, 241603. [CrossRef]
54. Reuter, M.; Saueressig, F. Renormalization group flow of quantum gravity in the Einstein–Hilbert truncation. *Phys. Rev.* **2002**, *D65*, 065016. [CrossRef]